Occurrence of Ambient Temperature and Reentrant Smectic Ordering in an Intermolecular Hydrogen Bonding between Alkyl Aniline and Alkoxy Benzoic Acids

T. Chitravel[a]; M. L. N. Madhu Mohan[a]

[a] Liquid Crystal Research Laboratory (LCRL), Bannari Amman Institute of Technology, Sathyamangalam, India

PLEASE SCROLL DOWN FOR ARTICLE

Taylor & Francis
Taylor & Francis Group

Occurrence of Ambient Temperature and Reentrant Smectic Ordering in an Intermolecular Hydrogen Bonding between Alkyl Aniline and Alkoxy Benzoic Acids

T. CHITRAVEL AND M. L. N. MADHU MOHAN

Liquid Crystal Research Laboratory (LCRL), Bannari Amman Institute of Technology, Sathyamangalam, India

A homologous series of inter-hydrogen-bonded complexes between p-n-alkoxybenzoic acids (12A + nBA) and alkyl aniline was isolated. The mesogenic p-n-alkoxybenzoic acids formed a hydrogen bond with liquid-crystal intermediate 4-dodecyl aniline. The isolated homologous series compounds were analyzed by Fourier transform infrared (FTIR), polarizing optical microscope, dielectric studies, and differential scanning calorimetry (DSC). An interesting feature of these homologous series was the occurrence of an ambient smectic ordering in some of the isolated mesogens. The phase diagrams of the p-n-alkoxybenzoic acids and the present homologous series were computed and compared. The hydrogen bond formation was evinced through FTIR spectral studies. Two higher member mesogens of the present homologous series were found to exhibit monotropic smectic G phase. Results of free p-n-alkoxybenzoic acids and the hydrogen-bonded homologous series are discussed in the light of increment alkoxy carbon number, mesogenic phases exhibited, and mesogenic thermal range.

Keywords Ambient smectic ordering; intermolecular hydrogen bonding; reentrant smectic ordering

Introduction

Liquid-crystal applications gained momentum after the discovery of the first ferroelectric liquid crystal by Meyer *et al.* [1]. Many research groups around the globe are working on hydrogen-bonded liquid crystals (HBLCs) [2–13]. These hydrogen-bonded ferroelectric liquid crystals (HBFLCs) are selected on the basis of their molecular reorganization and self-assembly capability. Tilt angle, spontaneous polarization, and optimum response times makes these materials lucrative for commercial applications [14–17]. These new types of soft covalent materials are now extensively investigated because they exhibit rich phase polymorphism

---

T. Chitravel is presently with Anna University, Tiruchirappalli, India.

Address correspondence to M. L. N. Madhu Mohan, Liquid Crystal Research Laboratory (LCRL), Bannari Amman Institute of Technology, Sathyamangalam 638 401, Tamilnadu, India. E-mail: mln.madhu@gmail.com

[5–13,18–22]. The reported data [5–13,18–22] indicate that if HBFLC materials are to be mesogenic, it is enough that either one of proton donor or acceptor molecules exhibits mesogenic property. The molecular structure [10,18–22] of HBLC is core-lated to the physical properties exhibited by it. Usually a hydrogen bond is formed between a proton donor and an acceptor group [2,7,10,13–21]. Discovery of hydrogen-bonded liquid crystal by Kato and Frechet [14] opened a new chapter in synthesis, design, and characterization of these mesogens, which facilitated many research groups [23–28] to work in this field.

With our previous experience [29–32] in designing and synthesizing liquid crystals and in continuation of our efforts to understand hydrogen-bonded mesogens, which were published as part I [33] and part II [34], in the present work a successful attempt has been made to design and isolate a homologous series of hydrogen-bonded liquid crystals with the aim of lowering the transition temperatures of the mesogens to the ambient temperatures. The mesogenic p-n-alkoxybenzoic acids (where n represents the alkoxy carbon number from 5 to 12 except 4 and 6) formed a hydrogen bond with liquid crystal intermediate 4-dodecyl aniline. Phase diagrams, mesogenic phase, and thermal range are discussed for the two different isolated homologous series.

Experimental

Materials and Instrumentation

Optical textural observations were made with a Nikon polarizing microscope equipped with a Nikon (Tokyo, Japan) digital CCD camera system with 5 mega pixels and 2560 * 1920 pixel resolutions. The liquid-crystalline textures were processed, analyzed, and stored with the aid of ACT-2U (Tokyo, Japan) imaging software system. The temperature control of the liquid-crystal cell was equipped by Instec HCS402-STC 200 temperature controller (Instec, Boulder, CO, USA) to a temperature resolution of $\pm 0.1^\circ C$. This unit is interfaced to a computer by IEEE-STC 200 to control and monitor the temperature. The liquid-crystal sample is filled by capillary action in its isotropic state into a untreated conducting cell with 4 μm spacer. The transition temperatures and corresponding enthalpy values were obtained by differential scanning calorimetry (DSC; Shimadzu DSC-60). The Fourier transform infrared (FTIR) spectra were recorded (ABB FTIR MB3000) and analyzed with the MB3000 software. The p-n-alkoxybenzoic acids (12A + nBA) and 4-dodecyl aniline were supplied by Sigma Aldrich (Seelze, Germany) and all the solvents used were E. Merck grade.

Synthesis of Intermolecular Hydrogen-Bonded Complexes

The intermolecular hydrogen-bonded complexes are synthesized by the addition of 2 mole of p-n-alkoxybenzoic acids (12A + nBA) with one mole of 4-dodecyl aniline in N,N-dimethyl formamide (DMF) respectively. Further, they are subject to constant stirring for 12 h at ambient temperature of 30°C until a white precipitate in a dense solution is formed. The white crystalline crude complexes so obtained by removing excess DMF by filtration are then recrystallized in dimethylsulfoxide (DMSO). The yields varied from 85 to 95%. The yield of higher homologues compounds is observed to be greater compared to its lower counterparts. The
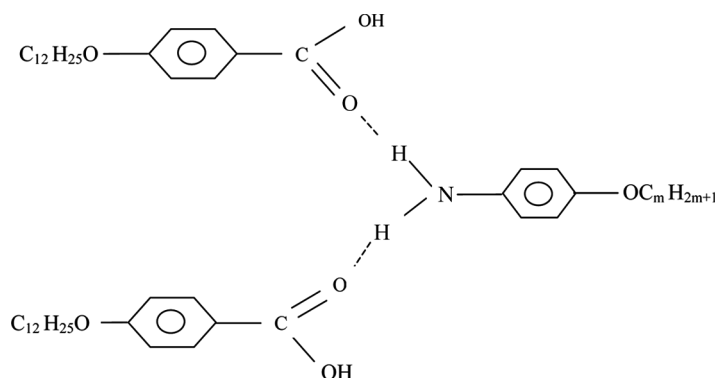
Figure 1. Molecular structure of dodecylaniline and alkoxy benzoic acid homologous series.

homologous series of p-n-alkoxybenzoic acids with 4-dodecyl aniline can be depicted as shown in Fig. 1, where n represents alkoxy carbon number of benzoic acid.

Results and Discussion

All the mesogens isolated under the present investigation are white crystalline solids and are stable at room temperature. They are insoluble in water and sparingly soluble in common organic solvents such as methanol, ethanol, benzene and dichloromethane. However, they show a high degree of solubility in coordinating solvents like DMSO, DMF and pyridine. All these mesogens melt at temperatures around 100°C (Table 1). They show high thermal and chemical stability when subjected to repeated thermal scans performed during thermal microscopy and DSC studies.

FT-IR Studies

The room temperature infrared (IR) spectrum of free alkoxy benzoic acids and its H-bonded complexes are recorded in solid state (KBr). The infrared frequencies of the pertinent bands are given in Table 1. The spectra of p-n-alkoxy benzoic acid show sharp bands at 1685 and 1695 cm^{-1} due to the ν(C=O) mode and a strong

Table 1. IR Spectral frequencies of pertinent bands

Compound	nBA moiety		Aniline moiety		
	ν(C=O)	ν(OH)	ν(C–O)	ν(N–H)	ν(>C=N–)
p-Dodecyloxy benzoic acid (CHCl$_3$)	1712	3012	—	—	—
Dodecyl aniline	—	—	1265	3371	1612
12A + 12(BA)$_2$	1682	2918	1258	3331	1608
12A + 11(BA)$_2$	1682	2916	1257	3325	1605
12A + 10(BA)$_2$	1682	2916	1257	3333	1605

intense band at $3012 \, \text{cm}^{-1}$ assigned to the $\nu(\text{OH})$ mode of the carboxylic acid group [35]. This doubling nature of the $\nu(\text{C=O})$ mode may be attributed to the dimeric nature of the acid group at room temperature [35]. The corresponding spectra in the solution state (chloroform) show a strong intense band at $1712 \, \text{cm}^{-1}$, suggesting the existence of the monomeric form of benzoic acid in the solution state. Comparison of the spectra of complexes is made with the solution spectra of free alkoxy benzoic acids.

The IR spectrum (KBr) of 4-dodecyl aniline shows characteristic bands for $\nu(\text{C=O})$ ($\sim 1612 \, \text{cm}^{-1}$), $\nu(\text{N–H})$ ($\sim 3371 \, \text{cm}^{-1}$), and $\nu(\text{C–O})_{\text{phenolic}}$ ($\sim 1265 \, \text{cm}^{-1}$) stretching modes [12]. The solid-state IR spectra of hydrogen-bonded complex $12A + (11BA)_2$ complex, as shown in Fig. 2, exhibit a sharp band at $1674 \, \text{cm}^{-1}$ with the disappearance of the doubling nature due to the $\nu(\text{C=O})$ mode of the benzoic acid moiety. This clearly suggests dissection of the dimeric p-n-alkoxy benzoic acids upon complexation.

Further, these complexes show bathochromic shifts in the $\nu(\text{C=O})$ ($\sim 30 \, \text{cm}^{-1}$) and $\nu(\text{OH})$ ($\sim 96 \, \text{cm}^{-1}$) modes of free alkoxy benzoic acid and the $\nu(\text{N–H})$ mode ($\sim 46 \, \text{cm}^{-1}$) group of aniline moiety, thereby indicating that both groups can form complementary H-bonding to accept as well as donate protons from one another [36]. The existence of the hydrogen bonding in the present series is further invoked by the bathochromic shift in the $\nu(\text{C–O})_{\text{phenolic}}$ mode of the aniline ($\sim 8 \, \text{cm}^{-1}$).

Phase Identification

The observed phase variants, transition temperatures, and corresponding enthalpy values obtained by DSC in cooling and heating run for the homologous series are presented in Table 2.
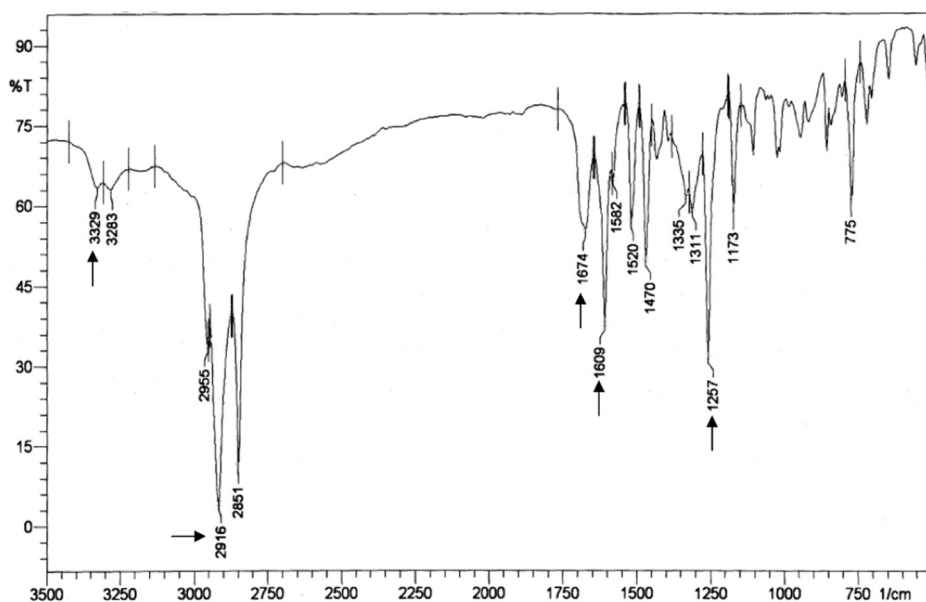

Figure 2. FTIR spectra of $12A + (11BA)_2$ hydrogen-bonded complex.

Table 2. Transition temperatures obtained by DSC of 12A + nBA homologous series. Enthalpy (ΔH) values are given in Joules/gram and temperature is measured in degrees centigrade

Carbon number	Phase variant	Technique	Crystal to melt	ΔH	C	ΔH	F	ΔH	G	ΔH	F_r	ΔH	Crystal	ΔH
3	G	DSC (h)	#	#									#	#
		DSC (c)							108.3	12.36				
		POM (c)							107.5					
5	G	DSC (h)	47.7	48.17										
		DSC (c)							64.7	77.24			29.8	42.56
		POM (c)							65.5				28.5	#
7	G	DSC (h)	#	#									#	#
		DSC (c)							88.3	10.60				
		POM (c)							89.5					
8	CFG	DSC (h)	74.3	21.49	96.7	0.32	95	0.88	*				44	26.69
		DSC (c)			91.3	Merged with F	89.5	16.94	45.1	Merged with crystal				
9	CFG	POM (c)			92.5		90.4		46.3				42.9	
		DSC (h)	93.4	64.04	104.1	0.20	*		*					
		DSC (c)			93.1	Not resolved	90.4	0.81	86.1	14.83			61.6	41.36
10	CFG	POM (c)			94.2		91.5		87.2				62.4	
		DSC (h)	34.6	9.29	96.2	4.94	93.5	3.49	86.7	13.51				
		DSC (c)	—		100.6	1.65	92.9	0.29	88.4	9.28	—		76.3	10.85
		POM (c)			101.4		93.8		89.6				77.6	
11	CFG	DSC (h)	35.3	26.28	100.2	3.18	80.2	13.82	74.1	10.19	—		40.1	32.83
		DSC (c)			101.5		81.6		75.4				41.2	
		POM (c)												
12	$CFGF_r$	DSC (h)	38.8	25.24	—		109.0	1.79	94.5	53.29	47.8	0.18	—	25.17
		DSC (c)			117.9	2.67	103.3	6.50	82.6	21.92	64.3	11.3	42.5	
		POM (c)			118.5		103.9		83.2		64.9		43.1	

#Room temperature liquid crystal.
*monotropic transition.

135

Dodecyl Aniline Benzoic Acids Homologous Series

The mesogens of the dodecyl aniline and benzoic acid homologous series on cooling from isotropic are found to exhibit characteristic textures [37], viz. smectic C (Schlieren texture, Plate 1) smectic F (broken focal conic texture, Plate 2), smectic G (multicolored mosaic texture, Plate 3), and smectic F reentrant (check board texture, Plate 4) phases, respectively. The general phase sequence of the dodecyl aniline and benzoic acid homologous series in the cooling run can be shown as:

$$\text{Isotropic} \rightarrow \text{Sm G} \rightarrow \text{Crystal} \qquad (\text{carbon number } 3, 5, \text{ and } 7)$$

$$\text{Isotropic} \rightarrow \text{Sm C} \rightarrow \text{Sm F} \rightarrow \text{Sm G} \rightarrow \text{Crystal} \qquad (\text{carbon number } 8 \text{ to } 11)$$

$$\text{Isotropic} \rightarrow \text{Sm C} \rightarrow \text{Sm F} \rightarrow \text{Sm G} \rightarrow \text{Sm F}_r \rightarrow \text{Crystal} \qquad (\text{carbon number } 12)$$

It is clearly evident from the above phase sequences that new smectic phases have been induced compared to pure benzoic acid homologous series. In other words, from carbon number 3 to 7, when compared to free alkoxy benzoic acid phase variance, in the present complex nematic of the pure alkoxybenzoic has been quenched and smectic G has been observed. Similarly, from carbon number 8, smectic F phase is induced. Thus, a good number of mesogenic phases have been induced in the lower and higher mesogens of the present series. Further, the complex 12 of the present series exhibits a reentrant smectic F ordering, which has been confirmed by DSC and optical textural studies. Two complexes, namely, octyl and nonyloxy benzoic acid complexes, exhibit monotropic smectic G transition where the smectic G phase is observed, in the heating cycle whereas it is not observed during the cooling cycle.

DSC Studies

DSC thermograms are obtained in heating and cooling cycles. The sample is heated with a scan rate of 10°C/min and held at its isotropic temperature for one minute to
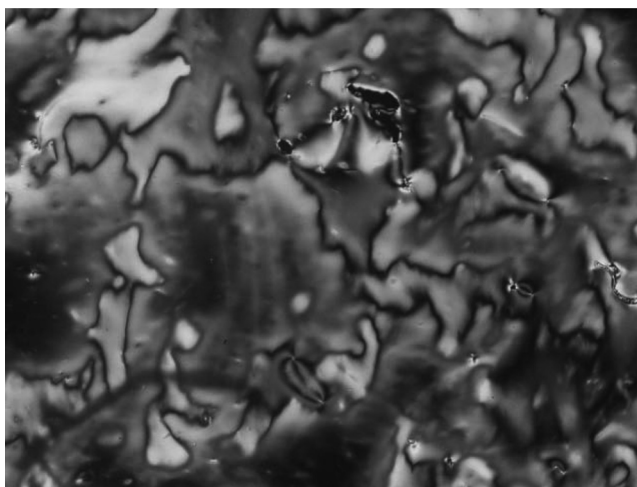

Plate 1. Schlieren texture of smectic C.

Plate 2. Broken focal conic texture of smectic F.

attain thermal stability. The cooling run is performed with a scan rate of $10°C/min$. The respective equilibrium transition temperatures and corresponding enthalpy values of the mesogens corresponding to the homologous series are listed separately in Table 2.

Reentrant Phenomenon

DSC Study. The phase transition temperatures and enthalpy values of dodecyloxybenzoic acid complex $[12A + (12BA)_2]$ are discussed. As shown in Fig. 3, in the cooling run the DSC thermogram exhibits five distinct transition temperatures. The phase, transition temperature, and enthalpy value in the cooling run of DSC are

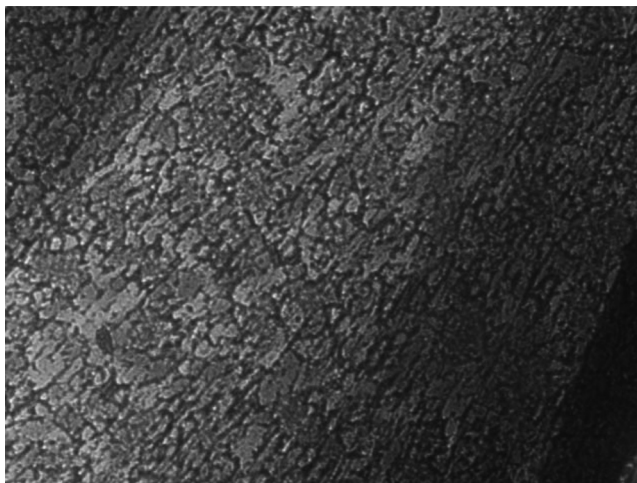**Plate 3.** Multicolored mosaic texture of smectic G.

Plate 4. Check-board texture of reentrant smectic F_r.

as follows: isotropic to smectic C (117.9°C, 2.67 J/g), smectic C to smectic F (103.3°C, 6.50 J/g), smectic F to smectic G (82.6°C, 21.92 J/g), smectic G to smectic F (reentrant); (64.3°C, 11.29 J/g), and smectic F (reentrant) to crystal (42.5°C, 25.17 J/g). In the heating cycle four distant transitions with enthalpy values are observed as crystal to melt (38.8°C, 25.24 J/g), melt to smectic F (reentrant); (47.8°C, 0.18 J/g), smectic F (reentrant) to smectic G (94.5°C, 53.29 J/g), smectic G to smectic F (109°C, 1.79 J/g). These transition temperatures and corresponding thermal spans of individual phases concur with polarizing optical microscopic (POM) studies.

Polarizing Optical Microscopy. The optical textural observations also confirm the reentrant DSC results. The phase sequence of the dodecyloxy benzoic acid
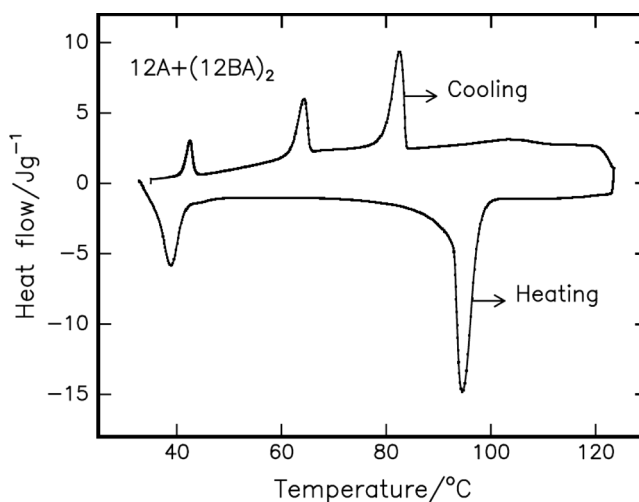

Figure 3. DSC thermogram of $12A + (12A)_2$ mesogen.

complex is cited above. Schlieren smectic C is observed, which transformed to broken focal conic texture of smectic F on further cooling smooth multicolored mosaic texture of smectic G is observed. Further cooling resulted in the reentrant smectic F with check-board texture as depicted in Plate 1.

Phase Diagrams

The phase diagrams of pure p-n-alkoxybenzoic acids and the dodecyl aniline homologous series are constructed through polarizing optical microscopic studies by the phase transition temperatures observed in the cooling run of the mesogens of the present homologous series. The phase diagram of pure p-n-alkoxybenzoic acids is composed of three tilted phases, namely, nematic, smectic C, and smectic G, as shown in Fig. 4.

From a close observation of the phase diagram of the complex illustrated in Fig. 5, the following observation are made.

All the mesogens of the present complex exhibit liquid crystallinity. Complexes 3 and 7 are found to exhibit wide thermal range of smectic G phase up to ~5°C, far beyond ambient temperatures. In general, smectic G phase is observed for the complexes with alkoxy carbon number 3 to 7, whereas smectic C, smectic F and smectic G phases are observed in complexes with alkoxy carbon number from 8 to 11. Smectic C, smectic F, and smectic G phases along with reentrant smectic F phases are observed for complex with alkoxy carbon number 12.

Smectic G phase is induced in the homologous series with alkyloxy carbon numbers from 3 to 9, and smectic F is induced in the complexes with alkyloxy carbon number 8 to 12. A reentrant smectic F is observed in dodecyl carbon complex with a wide thermal span. The mesogenic thermal span of the series is maximum from 3 to 7 alkoxy carbon numbers and minimum for nonyloxy hydrogen-bonded complex. In general the isotropic temperatures of the present series are much lower than the isotropic temperatures of the free alkoxy benzoic acids.

In the present study, as the alkoxy chain increases the variation of transition temperatures, specifically, the variation of the crystallization temperatures is
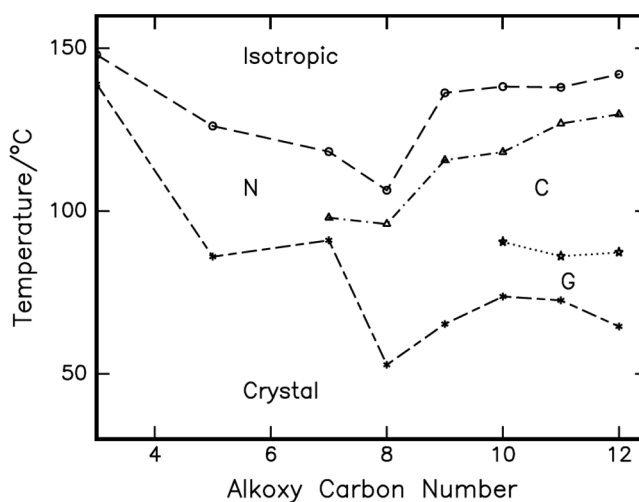

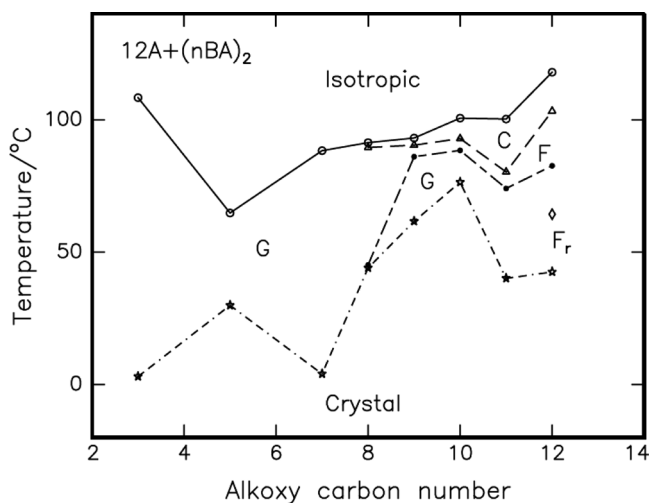**Figure 4.** Phase diagram of alkoxy benzoic acids.

Figure 5. Phase diagram of $12 + (nBA)_2$ hydrogen-bonded complex.

observed, which is attributed to the odd–even effect [38–42]. An odd–even effect is clearly observed in the present hydrogen-bonded complex phase diagram (Fig. 5) when compared to the pure alkoxy benzoic acid phase diagram (Fig. 4). In the present hydrogen complex homologous series, this odd–even effect has a pronounced influence on the crystallization temperatures; in other words, all the even complexes follow one pattern and the odd complexes follow yet another pattern. This result is in concurrence with the reported [38–42] literature on thermotropic liquid crystals. In the present homologous series, with the increase in the alkoxy carbon number beyond 6, induction of two new phases, namely, smectic G phase and reentrant smectic F_r phase, are observed. This is attributed to the changed structural configuration in the present homologous series. Addition of benzoic acids enhanced the conjugation, which in turn paved way for higher ionic flow; this could be the reason for inducement of higher order titled phases like smectic F and G. Reentrant nature is solely attributed to the changed molecular environment. The molecules flip their positions with decrement in temperature, causing the realignment. We already reported [43–46] several models in which various molecular orientations are suggested for reentrant phenomenon in hydrogen-bonded ferroelectric liquid crystals.

The pure alkoxy benzoic acid phase diagram (Fig. 4) depicts only three phases: nematic and two smectic phases, namely, C and G. The latter two smectic phases are observed when the alkoxy carbon number is equal to and greater than 7 and 10, respectively. The nematic and smectic C phase almost have a thermal span in the phase diagram. In the hydrogen-bonded complex phase diagram (Fig. 5) four smectic phases, namely, C, G, F, and reentrant F, are observed. It is further noticed that nematic, which appeared in the pure alkoxy phase diagram, is totally quenched by smectic G phase. Two new smectic phases, namely F and reentrant F, are induced in the phase diagram when the alkoxy carbon number is 8 to 12 and 12, respectively.

Dielectric Studies

Dielectric studies enable detecting second-order transitions that cannot be resolved by DSC studies. In the present study, as a representative case, $12A + (11BA)_2$

hydrogen-bonded complex is presented. This compound is filled in a untreated conducting cell of 4 μm spacer with an active area of 1 mm^2 under capillary action. Silver wires are drawn from the cell as leads. The empty cell (Instec, Boulder, CO, USA) is calibrated with temperature and with a known substance (benzene) (E. Merck, Germany) to calculate the leads' capacitance. The cell with the sample is placed in a Instec hot stage (HCS 402) whose temperature is monitored by a Instec stand-alone temperature controller (STC 200) interfaced with a computer, to an accuracy of $\pm 0.1^\circ$C. The sample is taken to its isotropic state and held for 2 min to attain thermal stability. Simultaneous textural observations are made to ascertain the phase of the mesogen. The readings are noted in the cooling run with a scan rate of 0.1°C/min. The 12A + (11BA)$_2$ compound in the cell is provided with a sinusoidal stimulus of 1.1 volt obtained from an HP 4192A impedance analyzer. The variation of the capacitance at two different frequencies, namely 10 and 100 KHz, is plotted in Fig. 6. From careful observation of Fig. 6 the following points are noted:

a) As the temperature is decreased from isotropic, smectic C phase is formed. This is manifested in the form of a small kink at 101.0°C in the dielectric spectrum.
b) In the entire thermal range of smectic C the capacitance value is unaltered, indicating the stabilization of the smectic C phase.
c) The sudden step-like decrement followed by a steep fall in the magnitude of the permittivity in the dielectric spectrum at 80.0°C is attributed to the onset of smectic F phase. From 80.0°C to 75.4°C, the thermal range of smectic F, the variation of capacitance is almost linear.
d) The onset of smectic G phase is seen in the dielectric spectrum as an anomaly at 75.4°C. In entire thermal range of smectic G the capacitance is unaltered, indicating the stabilization of the smectic G phase.
e) A sudden steep fall at 41.2°C in the magnitude of the permittivity indicates the onset of crystal.

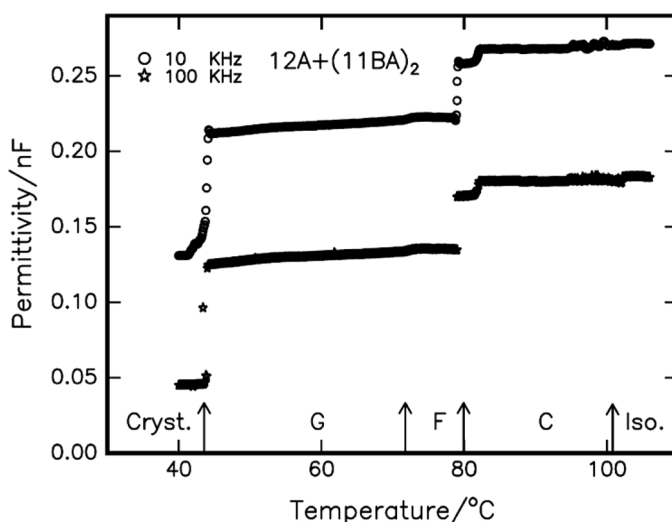**Figure 6.** Temperature variation of permittivity for 12A + (11BA)$_2$ mesogen at 10 and 100 KHz.

These variations in the magnitude of the permittivity are observed in both 10 and 100 KHz frequency spectra. Further, similar variations are noted in the dielectric loss spectrum pertaining to the corresponding frequencies. The transition temperatures obtained by this technique are in good agreement with those obtained from other techniques, namely, POM and DSC.

Conclusions

An inter-hydrogen-bonded liquid-crystalline complex between alkoxy benzoic acid and alkyl aniline has been successfully isolated and characterized. In comparison to the pure alkoxy benzoic acid phase diagram, in the present hydrogen-bonded complex, smectic G phase is observed to be induced in the lower homologous series with alkoxy carbon numbers 3 to 9 of the complex, whereas smectic F is observed to be induced in the rest of the series with alkoxy carbon numbers from 8 to 12. An interesting result is the observation of smectic reentrant F in hydrogen-bonded complex with alkoxy carbon number 12. DSC, dielectric, and textural studies confirm the above observations.

Acknowledgments

References

[1] Meyer, R. B., Liebert, L., Strzelecki, L., & Keller, P. (1975). *J. Phys. Lett.*, *36*, 69.
[2] Clark, N. A., & Lagerwall, S. T. (1980). *Appl. Phys. Lett.*, *36*, 899.
[3] Andersson, G., Dahl, I., Keller, P., Kuczynski, W., Lagerwall, S. T., Skarp, K., & Stebler, B. (1987). *App. Phys. Lett.*, *51*, 640.
[4] Gouda, F., Skarp, K., & Lagerwall, S. T. (1991). *Ferroelectrics*, *113*, 165.
[5] Andersson, G., Dahl, I., Kuczynski, W., Lagerwall, S. T., Skarp, K., & Stebler, B. (1988). *Ferroelectrics*, *84*, 285.
[6] Wang, J. M., Kim, Y. J., Kim, C. J., & Kim, K. S. (2002). *Ferroelectrics*, *277*, 185.
[7] Aira, H., Ray, H., & Kohki, T. (2004). *Jpn. J. Appl. Phys.*, *43*, 6243.
[8] Wu, S. L., & Lin, C. Y. (2003). *Liq. Cryst.*, *30*, 205.
[9] Kumar, P. A., & Pisipati, V. G. K. M. (2000). *Adv. Mater.*, *2*, 1617.
[10] Kittel, C. (1974). *Introduction to Solid State Physics*, Wiley Eastern Private Limited: New Delhi.
[11] Luckhurst, G. R., & Gray, G. W. (1979). *The Molecular Physics of Liquid Crystal*, Academic Press: New York.
[12] Niori, T., Sekine, T., Watanabe, J., Furukawa, T., Choi, S. W., & Takezoe, H. (1996). *J. Matter. Chem.*, *6*, 1231; (1997). *J. Mater. Chem.*, *7*, 1307.
[13] Adams, H., Braily, N. A., Bruce, D. W., Dhillon, R., Dunmur, D. A., Hunt, S. E., Lalinde, E., Maggs, A. A., Orr, R., Styring, P., Wragg, M. S., & Maitlies, P. M. (1988). *Polyhedron*, *7*, 1861.
[14] Kato, T., & Frechet, J. M. J. (1989). *J. Am. Chem. Soc.*, *111*, 8533.
[15] Kihara, H., Kato, T., Uryu, T., Ujiie, S., Kumar, U., Frechet, J. M. J., Bruce, D. W., & Price, D. J. (1996). *Liq. Cryst.*, *21*, 25.
[16] Brand, H. R., Cladis, P. E., & Pleiner, H. (1992). *Macromolecules*, *25*, 7223.

[17] Goodby, J. W., Blinc, R., Clark, N. A., Lagerwall, S. T., Osipov, M. A., Pikin, S. A., Sakurai, T., Yoshino, K., & Zeks, B. (1991). *Ferro Electric Liquid Crystal, Principles, Properties, and Applications*, Gordon and Breach Press: Philadalphia.

[18] de Gennes, P. G. (1974). *The Physics of Liquid Crystals*, Oxford Press: London.

[19] Sreedevi, B., Chalapathi, P. V., Srinivasulu, M., Pisipati, V. G. K. M., & Potukuchi, D. M. (2004). *Liq. Cryst.*, *31*, 303.

[20] Madhu Mohan, M. L. N., Goud, B. V. S., Kumar, P. A., & Pisipati, V. G. K. M. (1999). *Mater. Res. Bull.*, *34*, 2167.

[21] Noot, C., Perkins, S. P., & Coles, H. J. (2000). *Ferroelectrics*, *244*, 331.

[22] Chitravel, T., Madhu Mohan, M. L. N., & Krishnakumar, V. (2008). *Mol. Cryst. Liq. Cryst.*, *493*, 17.

[23] Letellier, P., Ewing, D. E., Goodby, J. W., Haley, J., Kelly, S. M., & Mackenzie, G. (1997). *Liq. Cryst.*, *22*, 609.

[24] Kumar, P. A., Srinivasulu, M., & Pisipati, V. G. K. M. (1999). *Liq. Cryst.*, *26*, 1339.

[25] Rudquist, P., Korblova, E., Walba, D. M., Shao, R., Clark, N. A., & Maclennan, J. E. (1999). *Liq. Cryst.*, *26*, 1555.

[26] Srinivasulu, M., Satyanarayana, P. V. V., Kumar, P. A., & Pisipati, V. G. K. M. (2001). *Liq. Cryst.*, *28*, 1321.

[27] Barmatov, E. B., Bobrovsky, A., Barmatova, M. V., & Shibaev, V. P. (1999). *Liq. Cryst.*, *26*, 581.

[28] Sideratou, Z., Tsiourvas, D., Paleos, C. M., & Skoulios, A. (1997). *Liq. Cryst.*, *22*, 51.

[29] Madhu Mohan, M. L. N., Arunachalam, B., & Arravindh Sankar, C. (2008). *Metall. Mater. Trans. A.*, *39*, 1192.

[30] Madhu Mohan, M. L. N., & Arunachalam, B. (2008). *Z. Naturforsch*, *63a*, 435.

[31] Pisipati, V. G. K. M., Kumar, P. A., & Madhu Mohan, M. L. N. (2000). *Mol. Cryst. Liq. Cryst.*, *350*, 141.

[32] Madhu Mohan, M. L. N., Kumar, P. A., & Pisipati, V. G. K. M. (2001). *Mol. Cryst. Liq. Cryst.*, *366*, 431.

[33] Vijayakumar, V. N., Murugadass, K., & Madhu Mohan, M. L. N. (2009). *Mol. Cryst. Liq. Cryst.*, *515*, 37.

[34] Madhu Mohan, M. L. N., & Pisipati, V. G. K. M. (2000). *Liq. Cryst.*, *26*, 1609.

[35] Nakamoto, K. (1978). *Infrared and Raman Spectra of Inorganic and Co-ordination Compounds*, Interscience: New York.

[36] Swathi, P., Kumar, P. A., Pisipati, V. G. K. M., Rajeswari, A. V., Sreehari Sastry, S., & Narayana Murty, P. (2002). *Z. Naturforsch.*, *57a*, 797.

[37] Gray, G. W., & Goodby, J. W. G. (1984). *Smectic Liquid Crystals: Textures and Structures*, Leonard Hill: London.

[38] Roviello, A., & Sirigu, A. (2003). *Makromol. Chem.*, *183*, 895.

[39] Marcelis, A. T. M., Koudijs, A., & Sudholter, E. J. R. (1995). *Liq. Cryst.*, *18*, 851.

[40] Pines, A., Ruben, D. J., & Allison, S. (1974). *Phys. Rev. Lett.*, *33*, 1002.

[41] Kuribayashi, M., & Hori, K. (1999). *Liq. Cryst.*, *26*, 809.

[42] Craig, A. A., & Imrie, C. T. (1995). *Macromolecules*, *28*, 3617.

[43] Vijayakumar, V. N., & Madhu Mohan, M. L. N. (2009). *Braz. J. Phys.*, in press.

[44] Vijayakumar, V. N., & Madhu Mohan, M. L. N. (2009). *Ferroelectrics*, *392*, 81.

[45] Vijayakumar, V. N., & Madhu Mohan, M. L. N. (2009). *Solid State Comm.*, *149*, 2090.

[46] Vijayakumar, V. N., Murugadass, K., & Madhu Mohan, M. L. N. (2009). *Braz. J. Phys.*, *39*, 600.